SAND2015-10856C

Hybrid fs/ps CARS for Sooting and Particle-laden Flames

Kathryn N. G. Hoffmeister,[1] Daniel R. Guildenbecher[2], and Sean P. Kearney[3]
Sandia National Laboratories, Albuquerque, New Mexico 87185

We report the application of ultrafast rotational coherent anti-Stokes Raman scattering (CARS) for temperature and relative oxygen concentration measurements in the plume emanating from a burning aluminized ammonium perchlorate propellant strand. Combustion of these metal-based propellants is a particularly hostile environment for laser-based diagnostics, with intense background luminosity, scattering and beam obstruction from hot metal particles that can be as large as several hundred microns in diameter. CARS spectra that were previously obtained using nanosecond pulsed lasers in an aluminum-particle-seeded flame are examined and are determined to be severely impacted by nonresonant background, presumably as a result of the plasma formed by particulate-enhanced laser-induced breakdown. Introduction of fs/ps laser pulses enables CARS detection at reduced pulse energies, decreasing the likelihood of breakdown, while simultaneously providing time-gated elimination of any nonresonant background interference. Temperature probability densities and temperature/oxygen correlations were constructed from ensembles of several thousand single-laser-shot measurements from the fs/ps rotational CARS measurement volume positioned within 3 mm or less of the burning propellant surface. Preliminary results in canonical flames are presented using a hybrid fs/ps vibrational CARS system to demonstrate our progress towards acquiring vibrational CARS measurements for more accurate temperatures in the very high temperature propellant burns.

Nomenclature

f	=	focal length
Φ	=	equivalence ratio
σ	=	standard deviation
τ	=	probe delay
T	=	temperature
v	=	vibrational quantum number
ω	=	wavenumber
Z	=	distance above burning surface

I. Introduction

UNDERSTANDING the complex, multiphase physics of burning solid rocket propellants is important to minimizing risks in fire scenarios. Metals, such as aluminum, are often added to solid rocket propellants to reduce combustion instabilities and increase specific impulse. The addition of aluminum also presents challenges to laser diagnostics in the form of smoky, two-phase flows created when aluminum particles agglomerate on the propellant surface and loft in the flow as large droplets up to 200 micrometers in diameter [1]. The burning of aluminized, solid rocket propellant creates hostile environments characterized by extremely high temperatures, background luminosity, background scattering, and beam obstruction from these molten metal particles. In these highly complex combustion environments, nonintrusive measurement techniques capable of probing multiphase flows are required to provide the spatially and temporally resolved thermochemical data needed to assess propellant

[1] Postdoctoral Fellow, Engineering Sciences Center, P.O. Box 5800/MS 0828, AIAA member.
[2] Senior Member of the Technical Staff, Engineering Sciences Center, P.O. Box 5800/MS 0840.
[3] Principal Member of the Technical Staff, Engineering Sciences Center, P.O. Box 5800/Mail Stop 0826, Associcate Fellow AIAA.

systems. Previously, planar laser-induced fluorescence has been applied to quantify the combustion of isolated aluminum drops [2, 3], but may be challenged in the more challenging environment created by the direct combustion of solid propellants. Alternatively, coherent anti-Stokes Raman scattering (CARS) is a potentially attractive approach for space- and time-resolved thermometry and species detection in theses hostile particle-laden environments. CARS is much more resilient to particle-induced optical interferences and has a strong history of application in soot-particle-laden flames [4-7], where other laser-based temperature diagnostics, such as Rayleigh and Raman scattering, often struggle.

While conventional, nanosecond CARS provides highly-accurate, spatially resolved, non-intrusive temperature and major species measurements, its applicability is limited in metal-burn environments. Applications of CARS to propellant combustion have included RDX decomposition [8] and combustion of SGP-38 [9]; Nitramines [10, 11]; and HNF [12] under a wide range of pressures. Raman signatures from a variety of combustion gases were observable, and the spectra were, in some cases, fit for both temperature and species. Analysis of these CARS spectra was quite often complicated by the presence of large nonresonant background contributions resulting from either high pressures and/or low concentration of the probed species. None of the propellants investigated with CARS were metallized, and interference from large-scale particulate did not appear to be a significant issue.

Coal combustion is perhaps the most similar system to metallized propellant in which CARS has been applied, with large-scale—10s to 100s of micron diameter—particulate present in these flames [13-16]. Nanosecond-duration laser pulses were used in all of these studies, and the pulse energies were several 10s of mJ in order to obtain single-laser-shot CARS detection. A key feature in all of these studies was the presence of significant nonresonant background in the measured spectra. This background intensity was comparable to, or even exceeded, the strength of the Raman-resonant N_2 signal of interest, significantly complicating the task of analyzing the spectra for quantitative temperature and species data. Beiting [13] provided a detailed investigation of the source of this nonresonant interference when coal-fly-ash particles of up to 50-μm size were present. He attributed the enhanced nonresonant susceptibility to plasma formation resulting from laser-induced dielectric breakdown in the CARS beam-crossing region. Beiting observed that the probability of breakdown scaled with both particle loading and laser pulse energy, which was confirmed in a later study of CARS measurements in coal-seeded flames by Hancock *et al.* [15]. Lucht [16] performed vibrational CARS of both N_2 and O_2 in a coal-particle-seeded methane/air flame. He was able to acquire spectra devoid of enhanced nonresonant background by limiting the pulse energies to 5 mJ in each of the three CARS laser beams. Good quality temperature measurements were obtained by averaging the signal for 50 – 100 laser shots, but signal yield was insufficient for single-laser-shot detection. When higher pulse energies were utilized, the spectra became contaminated by strong nonresonant background that was again attributed to laser-induced particle breakdown. This body of work shows that single-shot CARS thermometry, where pulse energies of 10s of mJ are often required, is difficult at best in the presence of large-scale particulate when nanosecond laser sources are employed.

We have attempted similar experiments using nanosecond vibrational CARS in an acetylene/air flame seeded with 10-μm-diameter aluminum particles. Representative spectra recorded with and without Al seeding are shown in Figure 1. With aluminum seed, the spectra were badly contaminated by intense nonresonant background and could not be further analyzed, as shown by the measurement at the top of Figure 1. In the absence of aluminum, good-quality CARS spectra, as displayed at the bottom of Figure 1, were readily measureable and fit to a theoretical prediction with a temperature of T = 2709 K, close to the adiabatic equilibrium temperature of 2773 K.

Recently, ultrafast CARS approaches have been developed for combustion sensing, primarily in clean

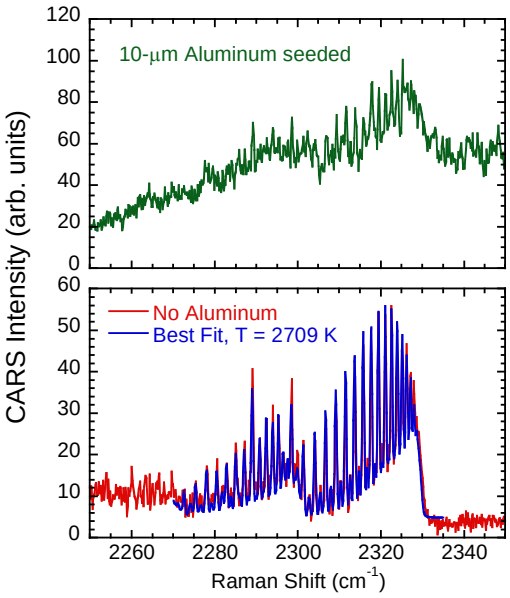

Figure 1: Nanosecond vibrational CARS spectra recorded from a C_2H_2/air flame. A best-case measured spectrum recorded from a flame seeded with 10-μm diameter aluminum particles is shown at top. At bottom, the red line represents the measured spectrum without aluminum seeding and the blue line represents the best-fit theoretical spectrum, returning a flame temperature of T = 2709 K.

laboratory flames [17-31], and are now beginning to see application in technical flame environments [32, 33]. Roy *et al.* [34] have recently applied an all picosecond ro-vibrational CARS setup for temperature measurements behind the blast wave generated by laser heating of aluminum nanoparticle samples pressed into ammonium-nitrate pellets, successfully observing post-shock temperatures in excess of 3500 K. The present study is believed to be the first application of ultrafast CARS to metallized propellant combustion, and is conducted with much larger sized metal particulate on the order of 10–100 μm. Femtosecond/picosecond CARS offers several distinct advantages for probing such particle-laden environments. The total pulse energy required for single-laser-shot detection can be 1 mJ or less, reducing the likelihood of laser-induced particle breakdown. In the event of breakdown, time gating provided by delay of the picosecond probe laser pulse [35-37] can be used to effectively eliminate the expected nonresonant background contamination of the signal. Finally, the sampling rate increases from the ~10-Hz level possible with nanosecond and picosecond Nd:YAG lasers to 1 kHz or better with commercial Ti:sapphire femtosecond amplifiers. This increased acquisition rate subsequently enhances the rate of valid spectra in which particulate do not obstruct the measurement volume [38].

In this study, we explore two types of fs/ps CARS. First, we apply pure-rotational fs/ps CARS to the metal-particle-laden plume emanating from a burning strand of aluminized ammonium perchlorate (AP) propellant. Traditionally, rotational CARS has been more accurate for low-temperature measurements where few vibrational levels are populated, and vibrational CARS is utilized at higher temperatures [25]. Based on the high temperatures measured by the pure-rotational fs/ps CARS system, 800 K to 3600 K, we have developed a fs/ps vibrational CARS instrument similar to that described by Miller *et al* [25], who have shown that long probe delays (τ >30 ps), can probe ground-state ro-vibrational levels for highly accurate low-temperature measurements [25], while maintaining the expected high-fidelity at high temperatures. In this study, we present initial results from our hybrid fs/ps vibrational CARS system, exploiting these long probe delays with the ultimate goal of acquiring propellant data accurate over the entire range of temperatures.

II. Experiments

A. Rotational fs/ps CARS facility

Rotational CARS spectra were acquired using the rotational fs/ps CARS facility described in detail in [29-31] and briefly summarized here. The rotational fs/ps CARS instrument is shown in Figure 2. A single-box Ti:sapphire chirped-pulse amplifier (Spectra Physics "Solstice") delivered a 1-kHz train of 800 nm, 90-100 fs pulses with a nominal bandwidth of 190 cm^{-1} (FWHM). Eighty percent of the 3.1 mJ pulse energy was used to generate a high-energy, 1-1.4 mJ, 5-ps-duration probe beam at 400 nm using the Second Harmonic Bandwidth Compression (SHBC Light Conversion) approach described in [30, 31]. The spectral width of the probe laser beam was 3.5 cm^{-1}. The remaining 20% of the compressed 800-nm femtosecond pulse was sent through a time-of-flight delay and split 50/50 to form separate pump and Stokes pulses, whose energies were regulated to ~100 μJ/pulse by a variable attenuator. Computer-controlled delay lines adjusted the relative delays of all three laser pulses to ensure proper sequencing in time. A 50-60 fs delay between the pump and Stokes pulses was introduced to optimize the performance of the CARS system at high temperatures, using the spectral focusing approach described in [29]. The 5-ps probe pulse was delayed by τ = 16 ps with respect to the pump/Stokes preparation pulses to provide time-gated elimination of any nonresonant CARS response, which is present only at zero delay [35, 36], as will be discussed in more detail below.

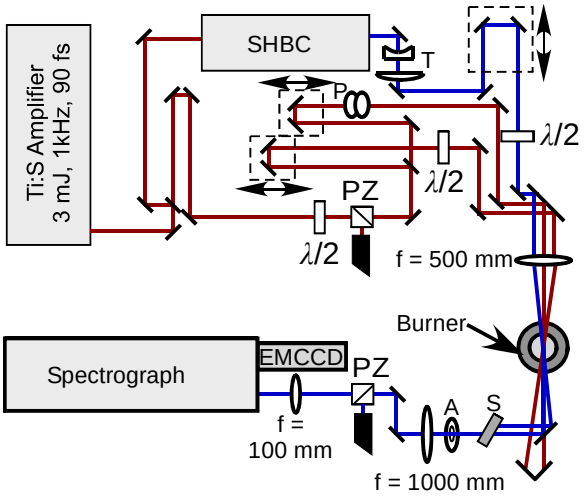

Figure 2: Schematic of the fs/ps rotational CARS instrument: f = lens focal length; λ/2 = half wave plate; PZ = polarizing cube; A = aperture; P = periscope; T = beam-expanding telescope; S = Semrock "razor edge" filter; SHBC = Second Harmonic Bandwidth Compressor; EMCCD = electron-multiplying CCD camera. Arrows indicate motion of computer-controlled delay stages.

A planar crossed-beam phase-matching scheme with an f = 500-mm beam-crossing lens was employed to generate the CARS signal beam in a nominally ellipsoidal measurement volume, with ~100-μm minor axis, and a major axis in which 90% of the CARS signal was generated in a 1.8-mm axial beam overlap region. The CARS signal was dispersed at ~0.95 cm^{-1}/pixel onto a back-illuminated, electron-multiplying CCD camera by a 1-m grating spectrograph with a grating groove density of 1800 mm^{-1}. Mie scattering of the probe laser line by large aluminum particles and small-diameter alumina smoke was particularly intense and was minimized using apertures along with a dielectric edge filter (Semrock "Razor Edge") [39] with a fast rise from the cutoff to the pass band in < 20 cm^{-1}.

B. Aluminized Propellant Burns

An aluminized propellant, nominally 70 weight% ammonium perchlorate (AP), 20 weight% aluminum particulate, and 10 weight% hydroxyl terminated polybutadiene binder, was formed into a pencil-like strand that was roughly 6-mm in diameter and 100-mm in length. The exterior strand surface was coated with an epoxy inhibitor, which promoted a downward propagating, nearly planar burn front that consumed the unreacted propellant. Aluminum agglomerates formed at the burning surface and were entrained into the resulting product gas plume. A still photograph extracted from the video recording of an experiment is shown in Figure 3, where the plume is observed to be intensely luminous with hot metal particulate and white smoke being ejected at the top. A detailed characterization of the aluminum particulate in these burning propellant samples has been provided via digital in-line holography (DIH) by Guildenbecher *et al.* [40]. Selected reconstructed holograms from a high-speed video recording of the near-surface particulate in a propellant burn experiment are shown in Figure 4a, while the measured probability density (pdf) of the particle size at a location that was nominally 10 mm above the burning surface is shown in Figure 4b. This number pdf is log-normal in nature, with Al particle sizes ranging from ten to several hundred microns. Representation of these data as a volume pdf reveals a bi-modal distribution, with a peak near 50 μm resulting from unagglomerated drops, and the larger peak at ~225 μm due to agglomerated aluminum particles [40].

Figure 3: Digital photograph of aluminized propellant strand burner flame.

The propellant strand was positioned so that the CARS measurement volume was placed just below its tip prior to ignition, with no CARS signal reaching the detector. Acquisition of single-laser-shot CARS spectra at 1 kHz was initiated just prior to ignition so that the first detected frames on the CCD camera were at background levels. The first detected CARS spectra arrived with the passing of the burning surface through the measurement volume, effectively marking a "zero time" for the measurements that was used with the known burn rate of 800 μm/s to estimate the distance from the surface to the CARS probe volume. The single-laser-shot CARS spectra were background subtracted and normalized by a nonresonant spectrum acquired in argon at zero probe-pulse delay to correct for the finite bandwidth of the femtosecond preparation pulses and collection optics. The measured spectra were dominated by N_2 and O_2, and were fit to the theoretical model described in [30, 31] for temperature and O_2/N_2 ratio.

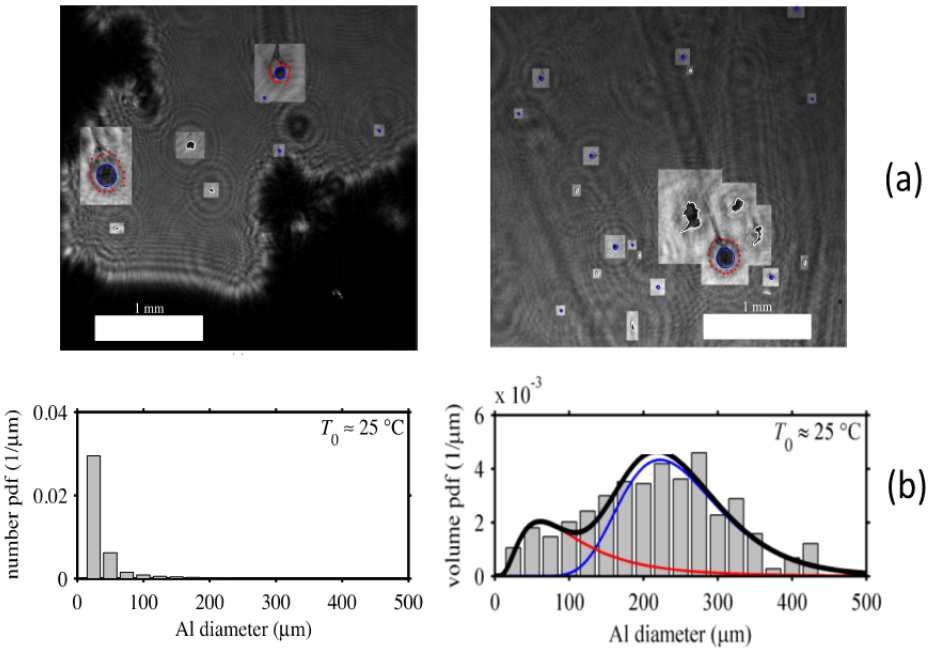

Figure 4: DIH characterization of aluminum particles [40]: representative holograms are provided in (a) while the size distribution is shown in (b).

C. Vibrational fs/ps CARS facility

Vibrational CARS spectra were acquired using a fs/ps CARS facility similar to the one described in [41]. The fs/ps CARS instrument is shown in Figure 5. A Ti:sapphire regenerative amplifier (Spectra Physics "Spitfire Ace HE") delivered a 2-kHz train of 6.5 mJ pulses centered at 800 nm. The 90-100 fs pulses had a nominal bandwidth of 190 cm^{-1} (FWHM) and were split into three portions. One portion is used to pump an optical parametric amplifier (TOPAS) to produce a 13-μJ pump beam centered at 675 nm. This pump beam was temporally overlapped with a second, 115-μJ portion of the initial 800-nm beam, which served as a Stokes source to prepare a vibrational Raman polarization in nitrogen. The third portion of the 800-nm, 100-fs beam was spectrally filtered by a Fabry-Perot etalon (455 cm^{-1} FSR) to create a 18-μJ, 1.5-ps probe beam with a ~5.3 cm^{-1} FWHM bandwidth (see Reference [42, 43]). Computer-controlled delay lines adjusted the relative delays of all three laser pulses to ensure proper sequencing in time.

A folded BOXCARS phase-matching scheme with an f = 500-mm beam-crossing lens was employed to generate the CARS signal beam in a nominally ellipsoidal measurement volume. Similar to the rotational CARS instrument, the CARS signal was dispersed at ~0.95 cm^{-1}/pixel onto a back-illuminated, electron-multiplying CCD camera by a 1-m grating spectrograph with a grating groove density of 1800 mm^{-1}.

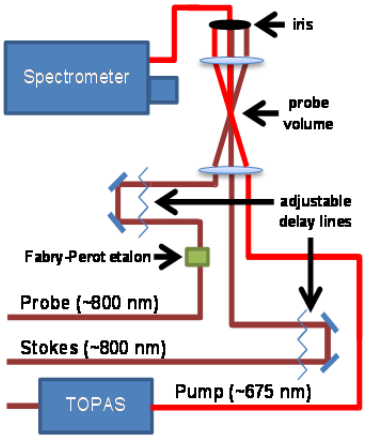

Figure 5: Schematic of the fs/ps vibrational CARS instrument.

D. Flat Flame Burners

Initial tests of the fs/ps vibrational CARS system were performed in Hencken [44] and McKenna [45] burners. A 50.8-mm square "Hencken" burner is used to create a series of well-characterized, near-adiabatic flames. The burner is operated with hydrogen/air mixtures, with hydrogen flow rates ranging from 7-45 SLPM (Φ = 0.3-1.2), and a constant air flow rate of 85.2 SLPM. Measurements were taken ~20 mm above the burner surface.

Measurement in the McKenna burner are based on a target flame identified by the International Workshop on Laser-induced Incandescence [46]. In this setup, a stabilization plate 60 mm in diameter and 20 mm thick sits 21 mm above the burner surface. The burner was run with a total gas flow of 10 SLPM and a nitrogen shroud of

~15 SLPM. For one set of measurements equivalence ratio was varied from .5 < Φ < 3.0 with measurements taken approximately 8.5 mm above the burner surface. In the second set of measurements, the equivalence ratio was fixed at 2.1 while the vertical profile of the temperature above the center of the burner cross section was investigated.

III. Results and Discussion

A. Rotational fs/ps CARS measurements in Aluminized Propellant Burns

Single-laser-shot rotational fs/ps CARS spectra were acquired for approximately 60 seconds following ignition for two different propellant strand burns. During the first 10 seconds (8 mm of surface regression) approximately 80% of the spectra displayed detectable signal-to-noise, defined here as peak detector counts of 500 or more above background. Loss of signal during the remaining 20% of the laser shots presumably arose from obscuration of the measurement volume by particulate, beam-steering effects, or low signal levels resulting from extremely high temperatures encountered near the burning propellant surface.

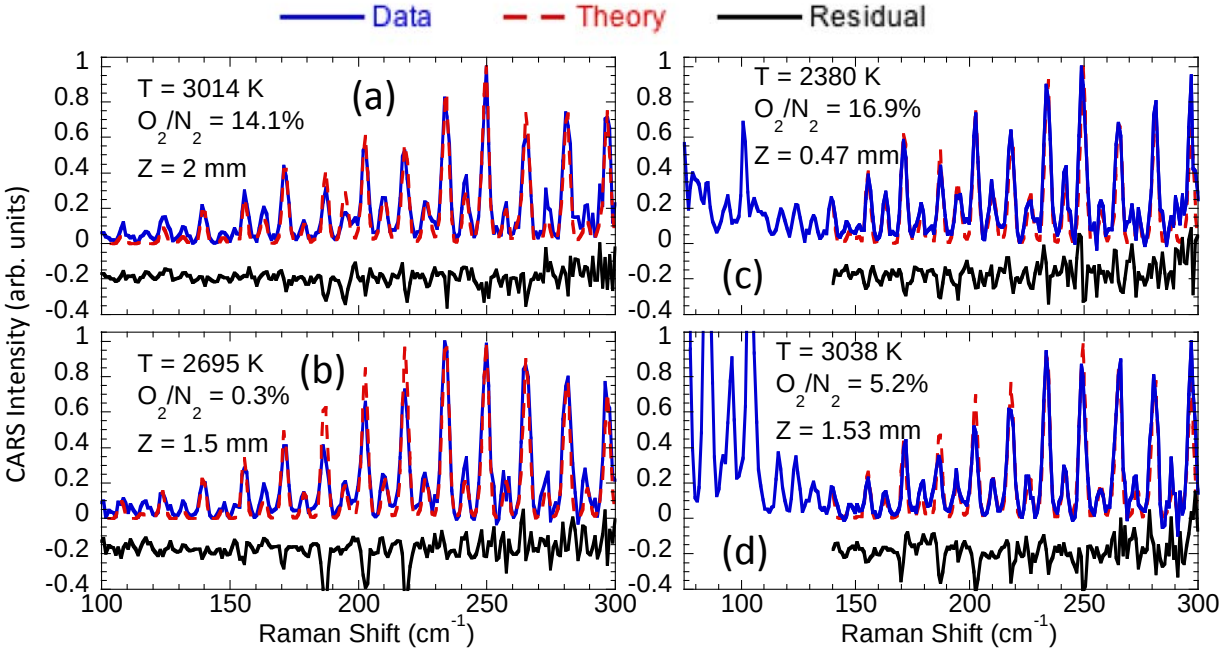

Figure 6: Representative single-laser-shot fs/ps pure-rotational CARS spectra obtained in the region 0.5-2.0 mm above the burning propellant surface. Spectra determined to arise primarily from high-temperature gases are shown on the left in (a, b), while results obtained with high gradients in the CARS measurement volume are shown at right in (c, d).

Representative single-laser-shot CARS spectra are shown along with the best-fit theoretical prediction and associated temperature and O_2/N_2 ratio in Figure 6. CARS intensities below 100 cm^{-1} were frequently impacted by intense scattering of the low-intensity wings of the probe laser line that was sufficiently strong to compete with the CARS spectrum at low frequencies. The necessary 100 cm^{-1} cutoff of the spectrum was acceptable because the intensity of low-frequency rotational transitions was small at the very high gas temperatures generated by aluminized AP combustion. The measured spectra could generally be classified as resulting from high-temperature gas only, as shown in Figure 6 a and b, or from both hot and cold gases simultaneously as a result of high thermal gradients along the 1.8-mm axis of the measurement volume, as in Figure 6 c and d. The effect of thermal gradients within the CARS measurement volume has been reported for nanosecond CARS spectra [47-49], where the cold-gas signal at low Raman shifts dominates the spectrum, with weaker intensity contributions from hot gases present at higher frequency. Spectra that were determined to be impacted by gradients were fit using the hot-gas-dominated, high-frequency portion of the spectrum, with Raman shifts ω = 140 – 300 cm^{-1}, in order to achieve a result that was indicative of the highest temperatures in the measurement volume. Spectra determined to be largely unimpacted by thermal gradients were fit using a wider spectral region of ω = 100 – 300 cm^{-1}.

The spectra in Figure 6 are free of nonresonant background of the type observed in Figure 1 in spite of what was likely the significant vaporization of aluminum particulate, as indicated by an audible tone at the 1-kHz laser

repetition rate that emanated from the propellant flame. Time-gated elimination of the nonresonant background is illustrated in Figure 7. The strength of the time-dependent Raman polarization calculated from expressions given in [30, 31] for O_2/N_2 = 5% at temperature T = 1650 K is shown in Figure 7a, as indicated by the blue line on the plot. Here, we can see the well-known [35, 36] nonresonant spike near time t = 0, which results from the electron polarizability and decays rapidly once the pump and Stokes pulses expire. The remaining elements of the Raman coherence at later time arise solely from the nuclear response of the probed molecules, and decay much more slowly. The effect of probe time delay is illustrated in Figure 7b and Figure 7c, where measured fs/ps rotational CARS spectra obtained in a premixed C_2H_4/air flame at T = 1650 K are shown. The spectrum in Figure 7b was obtained at probe delay τ = 0, and exhibits a significant nonresonant contribution. Introduction of the probe laser beam at τ = 16 ps delay results in a background-free spectrum, which is readily fit to the theoretical prediction, as illustrated in Figure 7c.

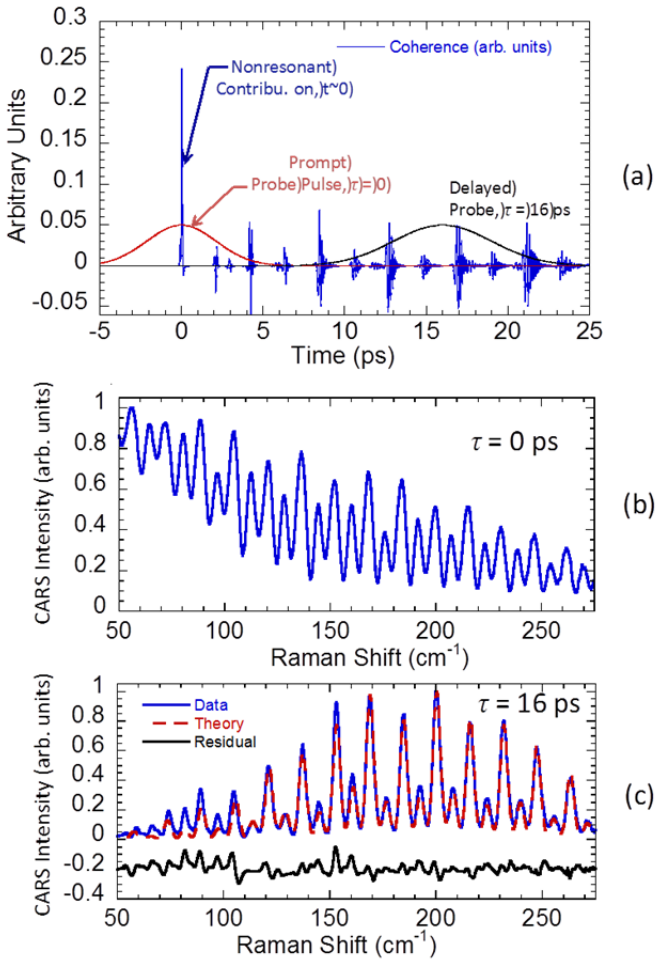

Figure 7: Time gating of the nonresonant background is illustrated. Calculated transient Raman response (blue line) at temperature T = 1650 K for an O_2/N_2 ratio of 5% is shown in part (a). Also shown in part (a) are 5-ps FWHM probe pulses introduced promptly with the pump and Stokes pulses, τ = 0, and delayed by τ = 16 ps as in our experiments. Nonresonant background, as measured in a premixed C_2H_4/air flame at zero delay is shown in (b), while a background-free spectrum from the same flame at τ = 16 ps is shown alongside a best-fit theoretical spectrum in (c).

Measured spectra from the aluminized AP propellant plume were dominated by contributions from N_2 and O_2, which were then the only species considered for fitting. Decomposition and burning of AP (NH_4ClO_4) produces major product species that may include H_2O, Cl_2, HCl, N_2O, NO, N_2, and O_2 [50, 51], while burning of the binder material will liberate additional products typical of hydrocarbon combustion such as H_2, CO, and CO_2. All of these species could potentially contribute to the rotational CARS spectrum. Rotational CARS signatures from H_2O are particularly weak [52], while the H_2 rotational spectrum is at Raman shifts of 350 cm^{-1} and higher, outside the detection bandwidth of our instrument. Selection of a τ = 16 ps probe delay minimized contributions from CO_2 and N_2O, whose nearest rotational Raman features are active at 21 and 19.9 ps, respectively. CO is has been included in our fs/ps CARS code, and results in only small perturbations on the measured spectrum due to its relatively low Raman cross section and the expected low concentrations here. The chlorine species were additionally added to our modeling code; however, the calculated spectral features did not become significant until concentrations reached levels comparable to N_2. These features were not observed in our measured spectra and thus determined to be weak. The only remaining species which remains to be checked were NO and N_2O, which may provide some perturbation to the measured spectra.

Significant O_2 content was observed throughout the plume over the nominal duration of the 60-second propellant burns. This was true even early in the experiments, when the CARS measurement volume was positioned close to the surface, so that mixing with room air is likely minimized, and the temperatures were very high, in excess of 2500 K in many cases. Indeed, the spectra shown in Figure 6a and Figure 6c reveal fit temperatures of T = 3014 K and 2380 K with significant O_2/N_2 mole-fraction ratios of 14.1% and 16.9%, respectively, such that high temperatures were attained with consumption of

minimal amounts of O_2, or with O_2 additionally present because it is a known product of AP deflagration.

Scatter plots of temperature vs. O_2/N_2 ratio were constructed from single-laser-shot measurements with the measurement volume within 3 mm (1/2 diameter) of the burning surface, with the results shown in Figure 8. Data from two different burns are shown with a conditionally averaged temperature drawn as solid lines through the data scatter. The conditionally averaged temperatures for the two experiments agree to within 3–10% across the full range of O_2 content. The conditional temperature for the second burn trends to a maximum near T = 2800 K at zero oxygen, while the curve below O_2/N_2 = 0.05 is flat, as a results of the potential for elevated O_2 content at high temperatures.

Temperature probability densities for heights $z \leq 3$ mm from the burning surface were estimated based on histograms of the CARS-measured temperatures, with the results shown in Figure 9. Mean temperatures for the two experiments are $\bar{T}$ = 2164 K and 2209 K, respectively, or within 2.1%. The shapes of the two temperature histograms are additionally quite similar, with the most probable temperature near T = 2400 – 2450 K, in good agreement with pyrometer-measured temperatures of T = 2400 – 2600 K reported for burns of larger,

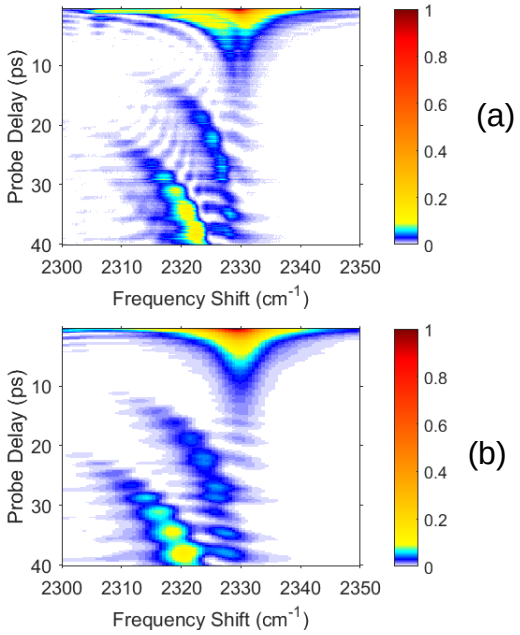

Figure 10: (a) Experimental and (b) theoretical time-dependence of fs/ps vibrational CARS spectra at 1300K. Experimental data measured in an open tube furnace

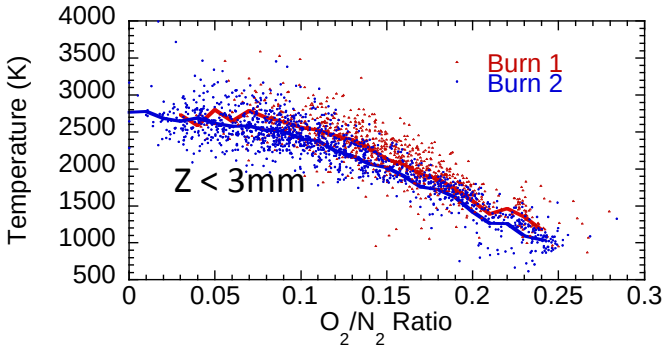

Figure 8: Temperature/oxygen scatter plot from fluctuations in the plume of the aluminized propellant strand burner.

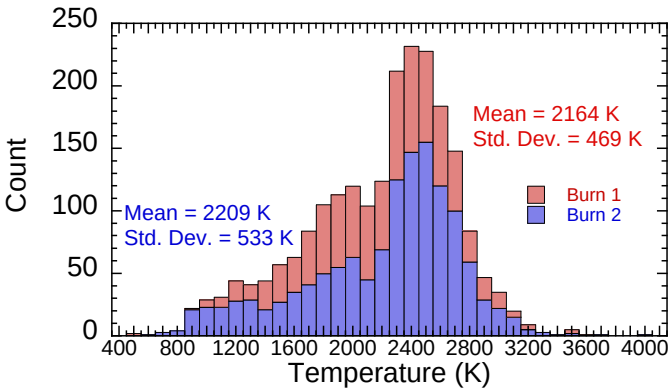

Figure 9: Probability density function of the temperature fluctuations in the plume of the aluminized propellant strand burner.

30-cm diameter slabs of similar aluminized AP propellant at ambient pressure [53].

B. Initial Results from Vibrational fs/ps CARS Instrument

In order to most accurately measure the large range of temperatures seen in Figure 9, a vibrational fs/ps CARS instrument was built. Based on the improvements to vibrational fs/ps CARS thermometry at low temperatures seen in [25], we performed a parametric study, measuring the CARS spectra while varying the probe delay time from $\tau = 0$ to 40 ps and temperature from 300 to 1300 K in an open-end tube furnace. Average experimental results (Figure 10, top) qualitatively agree with spectral shapes predicted from theory (Figure 10, bottom). Similar to the results seen by Miller *et al.* [25], while signal levels drop significantly with probe delay, they rebound near delays of τ = 30 ps. The experimental measurements at low probe delays contain a dual peak not seen in the theoretical spectra. This was determined to be due to an artifact in the probe pulse, which is remedied in the remainder of the measurements.

The average spectra (200 laser shots, 50 exposures) corresponding to τ = 20, 30, and 40 ps from Figure 10a were

fit to the theoretical spectra. The results are plotted versus measurements from a K-type thermocouple placed inside the furnace in Figure 12. With the exception of the room-temperature data, the fs/ps vibrational CARS temperatures match thermocouple data to within ± 5.5% across all probe delays.

In order to validate the system in clean-flame conditions, data were taken in the Hencken burner flame while the equivalence ratio was varied from Φ = .2 to 1.4. Each spectrum was averaged over 100 laser shots and spectra were recorded at probe-pulse delays of τ = 2 and 32.5 ps. The mean temperatures, calculated from fits to 100 shot-integrated spectra at each value of Φ, are plotted in Figure 12 with error bars representing 2σ. The red adiabatic flame curve represents equilibrium temperatures calculated using the NASA equilibrium code [54] minus 35 K (an estimate of the effects of heat loss to the burner surface).

For the τ = 2 ps case, the mean temperatures agree with the adiabatic flame temperatures to within 5.3% error except at lowest temperatures investigated. For temperatures below 1300 K, the error rapidly increases to 8.5% at Φ = .25 and 36.4% at Φ = .20. This increased error at low temperatures stems from a lack of structure in the vibrational CARS spectra at low temperatures and short probe delays (see Figure 13 below). In contrast, mean CARS temperatures for the τ = 32.5 ps case (probe delay used in [25]), agree with the adiabatic flame temperatures to within 4.8% over the entire range of stoichiometry investigated.

Having quantified the accuracy of vibrational fs/ps CARS measurements across a wide range of temperatures in clean, near-adiabatic flames, we demonstrate the system's capabilities in sooting-flame environments. Data were taken in a sooting, C_2H_4/air McKenna burner flame operated at Φ = 2.1. Example vibrational CARS temperature fits (from spectra averaged for 25 laser shots) are shown in Figure 13. Vibrational fs/ps CARS measurements taken while translating the measurement volume from the burner surface to the stabilization plate while at an equivalence ratio of Φ = 2.1 are shown in Figure 14, where the hybrid vibrational CARS temperature averages (with 2σ error bars), are plotted alongside measurements available in literature. The mean and standard deviation (error bars) are calculated from an ensemble of 300 measurements. Both the τ = 2 ps and τ = 32.5 ps temperatures between 5 and 10 mm agree to within ±4% of previous measurements taken using ns rotational CARS [55] and our fs/ps rotational CARS measurements [30]. However, temperatures near the stabilization plate in both the hybrid fs/ps rotational and vibrational CARS measurements taken in our laboratory are significantly (~10%) lower than those reported by Bohlin [55].

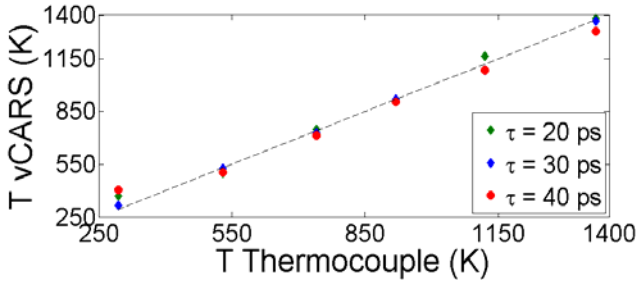

Figure 12: Vibrational fs/ps CARS temperature measurements vs thermocouple temperature readings of heated air in an open tube furnace.

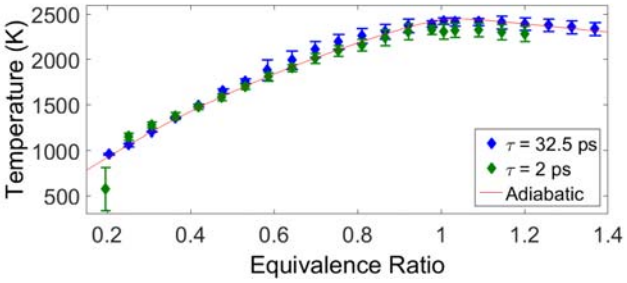

Figure 11: Vibrational fs/ps CARS temperature measurements vs equivalence ratio in a Hencken Burner. Temperatures in the adiabatic flame curve represent those calculated using the NASA CEA code [54] minus 35 K.

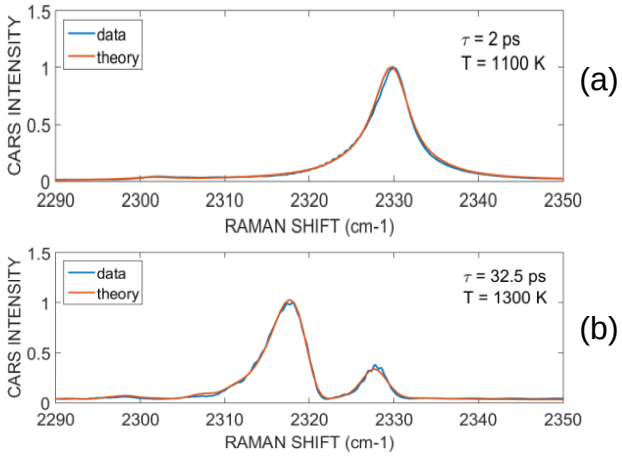

Figure 13: Sample vibrational fs/ps CARS spectra at probe delays of (a) τ = 2 ps and (b) τ = 32.5. Measurements collected over 100 laser shots.

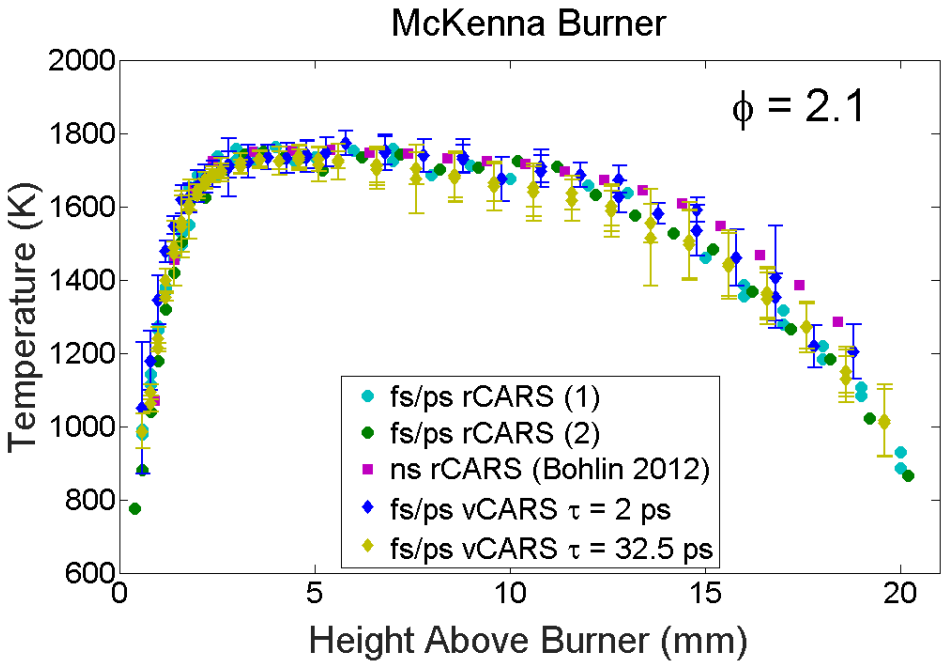

Figure 14: CARS temperature measurements vs height above McKenna Burner. Rotational fs/ps CARS measurements from [30]. Nanosecond rotational cars measurements from [55].

IV. Conclusion

We have applied a hybrid fs/ps rotational CARS instrument for measurements in the plume emanating from a burning strand of aluminized ammonium perchlorate propellant at atmospheric pressure. The loading of large, order 10-100 μm, aluminum particles in this flame presents an extreme challenge for CARS as well as other optical diagnostics, where significant background light scattering and a particularly troublesome nonresonant background can overwhelm the Raman-resonant spectroscopic signal of interest. Single-laser-shot spectra that were free of nonresonant background were successfully acquired throughout the plume, in some cases within 500 µm or less of the burning surface. Temperatures in excess of 3000 K were detected, with mean temperatures in the vicinity (≤ 3mm) of the surface near $T = 2200$ K.

The precision of a hybrid fs/ps vibrational CARS system was tested in well-characterized, flat-flame and furnace environments. Temperatures measured in an open-end tube furnace at time delays of $\tau = 20$, 30, and 40 ps agree to within 5.5% of thermocouple measurements for $T = 550$ to 1400 K. Using a time delay of $\tau = 32.5$ ps (from [25]), hybrid fs/ps vibrational CARS temperatures measured in a Hencken burner [44] agree to within 4.8% of expected near-adiabatic flame temperatures ranging from $T = 1000$ to 2400 K. Measurements in a sooting McKenna burner agree within ±5.5% of temperatures available in literature for locations away from the stabilization plate.

Future work will be directed at reducing of the 1.8-mm axial extent of the measurement volume to better resolve the large thermal gradients in these flames, and transitioning from rotational spectroscopy to vibrational CARS for the propellant temperature measurements, which may likely be a more sensitive thermometer at the very high temperatures, in excess of 3000 K, to be encountered. This will require the addition of a higher energy probe beam from the SHBC or a Nd:YAG regenerative amplifier [56] to generate sufficient signal for single-laser-shot measurements.

Acknowledgments

The authors thank Howard Lee Stauffacher for his handling and setup of the propellant strands. Sandia is a multiprogram laboratory operated by Sandia Corporation, a Lockheed-Martin Company, for the United States Department of Energy's National Nuclear Security Administration under Contract DE-AC04-94AL85000.

References

1. Price, E., and Sigman, R. "Combustion of aluminized solid propellants," *Solid propellant chemistry, combustion, and motor interior ballistics*. Vol. 185, American Institute of Aeronautics and Astronautics, Inc., Reston, VA, 2000, pp. 663-687.
2. Bucher, P., Yetter, R. A., Dryer, F. L., Parr, T. P., Hanson-Parr, D. M., and Vicenzi, E. P. "Flame structure measurement of single, isolated aluminum particles burning in air," *Twenty-Sixth Symposium (International) on Combustion* Vol. 26, No. 2, 1996, pp. 1899-1908.
3. Bucher, P., Yetter, R. A., Dryer, F. L., Parr, T. P., and Hanson-Parr, D. M. "PLIF species and ratiometric temperature measurements of aluminum particle combustion in O_2, CO_2, and N_2O oxidizers," *Twenty-Seventh Symposium (International) on Combustion* Vol. 27, No. 2, 1998, pp. 2421-2429.
4. Eckbreth, A. C., and Hall, R. J. "CARS Thermometry in a Sooting Flame," *Combustion and Flame* Vol. 36, 1979, pp. 87-98.
5. Kearney, S. P., and Jackson, M. N. "Dual-Pump CARS Thermometry in Heavily Sooting Flames," *AIAA Journal* Vol. 45, No. 12, 2007, pp. 2947-2956.
6. Beyrau, F., Seeger, T., Malarski, A., and Leipertz, A. "Determination of Temperatures and Fuel/Air Ratios in an Ethene-Air Flame by Dual-Pump CARS," *Journal of Raman Spectroscopy* Vol. 34, 2003, pp. 946-951.
7. Nordström, E., Olofsson, N. E., Simonsson, J., Johnsson, J., Bladh, H., and Bengtsson, P. E. "Local gas heating in sooting flames by heat transfer from laser-heated particles investigated using rotational CARS and LII," *Proceedings of the Combustion Institute* Vol. 35, 2015, pp. 3707-3713.
8. Aron, K., and Harris, L. E. "CARS probe of RDX decomposition," *Chemical Physics Letters* Vol. 103, No. 5, 1984, pp. 413-417.
9. Harris, L. E., and McIlwain, M. E. "Coherent anti-Stokes Raman temperature measurements in a propellant flame," *Combustion and Flame* Vol. 48, 1982, pp. 97-100.
10. Harris, L. E. "Hydrogen coherent anti-Stokes Raman spectra from CH_4-N_2O and nitramine composite flames," *Journal of the Chemical Society. Faraday Transactions 2* Vol. 82, No. 2129-2141, 1986.
11. Stufflebeam, J. H., and Eckbreth, A. C. "CARS diagnostics of solid propellant combustion at elevated pressure," *Combustion Science and Technology* Vol. 66, No. 163-179, 1989.
12. Dragomir, O. E., Tummers, M. J., Deen, E. H. v., Heijden, A. E. D. M. v. d., and Roekaerts, D. J. E. M. "Experimental investigation of the HNF flame structure," *Combustion and Flame* Vol. 153, 2008, pp. 149-160.
13. Beiting, E. J. "Coherent Interference in Multiplex CARS Measurements: Nonresonant Susceptibility Enhancement Due to Laser Breakdown," *Applied Optics* Vol. 24, No. 18, 1985, pp. 3010-3017.
14. Beiting, E. J. "Multiplex CARS Temperature Measurements in a Coal-Fired MHD Environment," *Applied Optics* Vol. 25, No. 10, 1986, pp. 1684-1692.
15. Hancock, R. D., Hedman, P. O., and Kramer, S. K. "Coherent anti-Stokes Raman spectroscopy (CARS) measurements in coal-seeded flames," *Combustion and Flame* Vol. 87, 1991, pp. 77-88.
16. Lucht, R. P. "Coherent anti-Stokes Raman scattering measurements in coal-particle-laden flames, SAND88-8721." Sandia National Laboratories, Livermore, CA, 1988.
17. Lang, T., and Motzkus, M. "Single-shot femtosecond coherent anti-Stokes Raman-scattering thermometry," *Journal of the Optical Society of America B* Vol. 19, No. 2, 2002, pp. 340-344.
18. Lucht, R. P., Roy, S., Meyer, T. R., and Gord, J. R. "Femtosecond Coherent Anti-Stokes Raman Scattering Measurement of Gas Temperatures from Frequency-Spread Dephasing of the Raman Coherence," *Applied Physics Letters* Vol. 89, 2006, p. 251112.
19. Kulatilaka, W. D., Stauffer, H. U., Gord, J. R., and Roy, S. "One-Dimensional Single-Shot Thermometry in Flames Using Femtosecond-CARS Line Imaging," *Optics Letters* Vol. 36, No. 21, 2011, pp. 4182-4184.
20. Roy, S., Kulatilika, W. D., Richardson, D. R., Lucht, R. P., and Gord, J. R. "Gas-Phase Single-Shot Thermometry at 1 kHz Using fs-CARS Spectroscopy," *Optics Letters* Vol. 34, No. 24, 2009, pp. 3587-3589.
21. Miller, J. D., Dedic, C. E., Meyer, T. R., Roy, S., and Gord, J. R. "Rotational fs/ps CARS for *in situ* Temperature and Concentration Measurements AIAA 2012-1192." 2012.
22. Miller, J. D., Dedic, C. E., Roy, S., Gord, J. R., and Meyer, T. R. "Interference-Free Gas-Phase Thermometry at Elevated Pressure Using Hybrid Femtosecond/Picosecond Rotational Coherent Anti-Stokes Raman Scattering," *Optics Express* Vol. 20, No. 5, 2012, pp. 5003-5010.
23. Miller, J. D., Roy, S., Slipchenko, M. N., Gord, J. R., and Meyer, T. R. "Single-Shot Gas-Phase Thermometry Using Pure-Rotational Hybrid Femtosecond/Picosecond Coherent anti-Stokes Raman Scattering," *Optics Express* Vol. 19, No. 16, 2011, pp. 15627-15640.

24. Miller, J. D., Slipchenko, M. N., Meyer, T. R., Stauffer, H. U., and Gord, J. R. "Hybrid Femtosecond/Picosecond Coherent Anti-Stokes Raman Scattering for High-Speed Thermometry," *Optics Letters* Vol. 35, No. 14, 2010, pp. 2430-2432.
25. Miller, J. D., Dedic, C. E., and Meyer, T. R. "Vibrational femtosecond/picosecond coherent anti-Stokes Raman scattering with enhanced temperature sensitivity for flame thermometry from 300 to 2400 K," *Journal of Raman Spectroscopy* Vol. 46, No. 8, 2015, pp. 702-707.
26. Dedic, C. E., Miller, J. D., and Meyer, T. R. "Dual-pump vibrational/rotational femtosecond/picosecond coherent anti-Stokes Raman scattering temperature and species measurements," *Optics Letters* Vol. 39, No. 23, 2014, pp. 6608-6611.
27. Bohlin, A., and Kliewer, C. J. "Diagnostic imaging in flames with instantaneous planar coherent Raman spectroscopy," *The Journal of Physical Chemistry Letters* Vol. 5, 2014, pp. 1242-1248.
28. Bohlin, A., and Kliewer, C. J. "Single-shot hyperspectral coherent Raman planar imaging in the range 0-4200 cm^{-1}," *Applied Physics Letters* Vol. 105, 2014, p. 161111.
29. Kearney, S. P. "Bandwidth optimization of femtosecond pure-rotational coherent anti-Stokes Raman scattering by pump/Stokes spectral focusing," *Applied Optics* Vol. 53, No. 28, 2014, pp. 6579-6585.
30. Kearney, S. P. "Hybrid fs/ps rotational CARS temperature and oxygen measurements in the product gases of canonical flat flames," *Combustion and Flame* Vol. 162, 2015, pp. 1748-1758.
31. Kearney, S. P., and Scoglietti, D. J. "Hybrid femtosecond/picosecond rotational coherent anti-Stokes Raman scattering at flame temperatures using a second-harmonic bandwidth-compressed probe," *Optics Letters* Vol. 38, No. 6, 2013, pp. 833-835.
32. Bohlin, A., Mann, M., Patterson, B. D., Dreizler, A., and Kliewer, C. J. "Development of two-beam femtosecond/picosecond one-dimensional rotational coherent anti-Stokes Raman spectroscopy: Time-resolved probing of flame wall interactions," *Proceedings of the Combustion Institute* Vol. 35, 2015, pp. 3723-3730.
33. Dennis, C. N., Slabaugh, C. D., Boxx, I. G., Meier, W., and Lucht, R. P. "Chirped probe pulse femtosecond coherent anti-Stokes Raman scattering at 5 kHz in a Gas Turbine Model Combustor," *Proceedings of the Combustion Institute* Vol. 35, No. 3, 2014, pp. 3731-3738.
34. Roy, S., Jiang, N., Stauffer, H. U., Schmidt, J. S., Kulatilika, W. D., Meyer, T. R., Bunker, C. E., and Gord, J. R. "Spatially and temporally resolved temperature and shock-speed measurements behind a laser-induced blast wave of energetic nanoparticles," *Journal of Applied Physics* Vol. 113, 2013, p. 184310.
35. Meyer, T. R., Roy, S., and Gord, J. R. "Improving signal-to-interference ratio in rich hydrocarbon–air Flames using picosecond coherent anti-Stokes Raman scattering," *Applied Spectroscopy* Vol. 61, No. 11, 2007, pp. 1135-1140.
36. Roy, S., Meyer, T. R., and Gord, J. R. "Time-Resolved Dynamics of Resonant and Nonresonant Broadband Picosecond Coherent Anti-Stokes Raman Scattering Signals," *Applied Physics Letters* Vol. 87, No. 26, 2005, p. 264103.
37. Miller, J. D., Slipchenko, M. N., and Meyer, T. R. "Probe-pulse optimization for nonresonant suppression in hybrid fs/ps coherent anti-Stokes Raman scattering at high temperature," *Optics Express* Vol. 19, No. 14, 2011, pp. 13326-13333.
38. Gord, J. R., Meyer, T. R., and Roy, S. "Applications of Ultrafast Lasers for Optical Measurements in Combusting Flows," *Annual Review of Analytical Chemistry* Vol. 2008, No. 1, 2008, pp. 663-687.
39. Bohlin, A., and Bengtsson, P. E. "Effective suppression of stray light in rotational coherent anti-Stokes Raman spectroscopy using an angle-tuned short-wave-pass filter," *Applied Spectroscopy* Vol. 64, No. 8, 2010, pp. 964-966.
40. Guildenbecher, D. R., Cooper, M. A., Gill, W., Stauffacher, H. L., Oliver, M. S., and Grasser, T. W. "Quantitative, three-dimensional imaging of aluminum drop combustion in sold propellant plumes via digital in-line holography," *Optics Letters* Vol. 39, No. 17, 2014, pp. 5126-5129.
41. Miller, J. D., Slipchenko, M. N., Meyer, T. R., Stauffer, H. U., and Gord, J. R. "Hybrid femtosecond/picosecond coherent anti-Stokes Raman scattering for high-speed gas-phase thermometry," *Optics Letters* Vol. 35, No. 14, 2010, pp. 2430-2432.
42. Stauffer, H. U., Miller, J. D., Roy, S., Gord, J. R., and Meyer, T. R. "Hybrid Femtosecond/Picosecond Rotational Coherent Anti-Stokes Raman Scattering Using a Narrowband Time-Asymmetric Probe Pulse," *The Journal of Chemical Physics* Vol. 136, 2012, p. 111101.
43. Lagutchev, A., Hambir, S. A., and Dlott, D. D. "Nonresonant Background Suppression in Broadband Vibrational Sum-Frequency Generation Spectroscopy," *Journal of Physcial Chemistry C* Vol. 111, 2007, pp. 13645-13647.
44. Hancock, R. D., Bertagnolli, K. E., and Lucht, R. P. "Nitrogen and hydrogen CARS temperature measurements in a hydrogen/air flame using a near-adiabatic flat-flame burner," *Combustion and Flame* Vol. 109, No. 3, 1997, pp. 323-331.
45. Senser, D. W., Morse, J. S., and Cundy, V. A. "Construction and novel application of a flat flame burner facility to study hazardous waste combustion," *Review of Scientific Instruments* Vol. 56, No. 6, 1985, pp. 1279-1284.
46. http://liiscience.org/target_flames.
47. Zhu, J. Y., and Dunn-Rankin, D. "CARS Thermometry in High Temperature Gradients," *Applied Physics B* Vol. 56, 1993, pp. 47-55.
48. Boquillon, J. P., Péalat, M., Bouchardy, P., Collin, G., Magre, P., and Taran, J. P. "Spatial averaging and multiplex coherent anti-Stokes Raman scattering temperature-measurement error," *Optics Letters* Vol. 13, No. 9, 1988, pp. 722-724.

49. Gao, Y., Seeger, T., and Leipertz, A. "Development of temperature evaluation of pure Rotational Coherent Anti-Stokes Raman Scattering (RCARS) spectra influenced by spatial averaging effects," *Proceedings of the Combustion Institute* Vol. 35, No. 3, 2015, pp. 3715-3722.
50. Keenan, A. G., and Siegmund, R. F. "Thermal decomposition of ammonium perchlorate," *Quarterly Reviews, Chemical Society* Vol. 23, No. 3, 1969, pp. 430-452.
51. Ermolin, N., Korobeinichev, O., Tereshchenko, A., and Fomin, V. "Measurement of the concentration profiles of reacting components and temperature in an ammonium perchlorate flame," *Combustion, Explosion, and Shock Waves* Vol. 18, No. 1, 1982, pp. 36-38.
52. Nordström, E., Bohlin, A., and Bengtsson, P. E. "Pure rotational coherent anti-Stokes Raman spectroscopy of water vapor and its relevance for combustion diagnostics," *Journal of Raman Spectroscopy* Vol. 44, No. 1322-1325, 2013.
53. Height, J. L., Donaldson, B. A., Gill, W., and Parigger, C. G. "Measurements in solid propellant plumes at ambient conditions, IMECE2011-62726," *ASME International Mechanical Engineering Congress and Exposition*. Denver, CO, 2011.
54. McBride, B. J., and Gordon, S. "Computer program for calculation of complex chemical equilibrium compositions and applications: II. Users manual and program description," *NASA reference publication* Vol. 1311, 1996, pp. 84-85.
55. Bohlin, A. "Development and application of pure rotational CARS for reactive flows, Ph.D. Thesis," *Division of Combustion Physics*. Vol. Ph.D., Lund University, 2012.
56. Bohlin, A., Patterson, B. D., and Kliewer, C. J. "Simplified two-beam rotational CARS signal generation demonstrated in 1D," *The Journal of Chemical Physics* Vol. 138, 2013, p. 081102.